References and Notes

1. A. H. Knoll *et al.*, *Earth Planet. Sci. Lett.* **240**, 179 (2005).
2. S. W. Squyres *et al.*, *Science* **306**, 1709 (2004).
3. G. Klingelhöfer *et al.*, *Science* **306**, 1740 (2004).
4. S. M. McLennan *et al.*, *Earth Planet. Sci. Lett.* **240**, 95 (2005).
5. J. P. Grotzinger *et al.*, *Earth Planet. Sci. Lett.* **240**, 11 (2005).
6. A. Gendrin *et al.*, *Science* **307**, 1587 (2005).
7. J. C. Bridges, M. M. Grady, *Earth Planet. Sci. Lett.* **176**, 267 (2000).
8. D. W. Ming *et al.*, *J. Geophys. Res. Planets* **111**, E02S12 (2006).
9. At equilibrium, the vapor pressure of water above an aqueous solution is equal to p_{aq}. For pure water at a standard state, the vapor pressure is equal to p_l^0. The activity of the solvent water, a_{H_2O}, is given by $a_{H_2O} = \frac{p_{aq}}{p_l^0}$.
10. W. D. Grant, *Philos. Trans. R. Soc. London Ser. B* **359**, 1249 (2004).
11. The food industry has expended considerable effort to characterize biological limits to a_{H_2O} in order to retard spoilage by microbial growth. The paucity of organisms found at low a_{H_2O} represents biological limitation rather than sampling or research bias.
12. Methods are described in the SOM text.
13. L. A. Hardie, H. P. Eugster, *Mineral. Soc. Am. Spec. Pub.* **3**, 273 (1970).
14. N. J. Tosca *et al.*, *Earth Planet. Sci. Lett.* **240**, 122 (2005).
15. N. J. Tosca *et al.*, *J. Geophys. Res. Planets* **109**, E05003 (2004).
16. Our calculations simulate the evaporation of a dilute basaltic-weathering derived fluid. Equilibrium with a 1-bar CO_2 atmosphere is maintained; the SO_4/Cl is specified; and pH, initially 3.9 unless otherwise stated, is calculated by charge balance.
17. Sedimentary redistribution may complicate estimations of a_{H_2O} for specific localities.
18. G. M. Marion, J. S. Kargel, *Cold Aqueous Geochemistry with FREZCHEM* (Springer-Verlag, Berlin, 2008).
19. B. C. Clark *et al.*, *Earth Planet. Sci. Lett.* **240**, 73 (2005).
20. N. J. Tosca, S. M. McLennan, *Earth Planet. Sci. Lett.* **241**, 21 (2006).
21. Relative humidity (RH) or brine chemistry may affect the hydration state of some evaporitic minerals. Here we exclude postdepositional RH effects and consider only fluid evaporation.
22. R. C. Peterson, R. Y. Wang, *Geology* **34**, 957 (2006).
23. A. H. Knoll *et al.*, *J. Geophys. Res. Planets* **113**, E06S16 (2008).
24. J. M. Keller *et al.*, *J. Geophys. Res. Planets* **111**, E03S08 (2006).
25. M. M. Osterloo *et al.*, *Science* **319**, 1651 (2008).
26. J. R. Johnson *et al.*, *Geophys. Res. Lett.* **34**, L13202 (2007).
27. Mössbauer spectra show that candidate minerals must be Fe-sulfates distinct from jarosite. At such highly concentrated and acidic conditions, the a_{H_2O} is relatively insensitive to the exact Fe-sulfate phase (see SOM).
28. A. Oren, *J. Ind. Microbiol. Biotechnol.* **28**, 56 (2002).
29. M. E. Elwood-Madden, R. J. Bodnar, J. D. Rimstidt, *Nature* **431**, 821 (2004).
30. J. A. Hurowitz, S. M. McLennan, *Earth Planet. Sci. Lett.* **260**, 432 (2007).
31. J. C. Andrews-Hanna, R. J. Phillips, M. T. Zuber, *Nature* **446**, 163 (2007).
32. M. H. Carr, *The Surface of Mars* (Cambridge Univ. Press, New York, 2007).

33. We thank the MER science and engineering teams for measurements of martian materials that made this paper possible. Research supported in part by NASA and a Harvard Origins postdoctoral fellowship to NJT.

Supporting Online Material

www.sciencemag.org/cgi/content/full/320/5880/1204/DC1
SOM Text
Figs. S1 to S4
Tables S1 to S6
References

18 January 2008; accepted 18 April 2008
10.1126/science.1155432

A Cytosolic Iron Chaperone That Delivers Iron to Ferritin

Haifeng Shi,[1] Krisztina Z. Bencze,[2] Timothy L. Stemmler,[2] Caroline C. Philpott[1]*

Ferritins are the main iron storage proteins found in animals, plants, and bacteria. The capacity to store iron in ferritin is essential for life in mammals, but the mechanism by which cytosolic iron is delivered to ferritin is unknown. Human ferritins expressed in yeast contain little iron. Human poly (rC)–binding protein 1 (PCBP1) increased the amount of iron loaded into ferritin when expressed in yeast. PCBP1 bound to ferritin in vivo and bound iron and facilitated iron loading into ferritin in vitro. Depletion of PCBP1 in human cells inhibited ferritin iron loading and increased cytosolic iron pools. Thus, PCBP1 can function as a cytosolic iron chaperone in the delivery of iron to ferritin.

Ferritins are iron storage proteins that are ubiquitously expressed in animals, plants, and bacteria. They serve both to sequester excess iron taken up by the cell and to release stored iron to meet the cell's metabolic needs during iron scarcity (*1*). In animals, ferritin is a cytosolic heteropolymer consisting of 24 subunits of heavy (H) and light (L) isoforms that assemble into a hollow sphere into which iron is deposited. Ferritin H chains contain the iron-binding and ferroxidase activities that are required for mineralization of the ferritin core. Deletion of the H-ferritin gene is lethal in mice (*2*) and in flies (*3*).

In cells, metallochaperones deliver metals to their cognate enzymes and transporters. Although cytosolic copper and nickel chaperones have been described (*4*–*7*), no cytosolic iron chaperones have been identified, despite the presence of numerous iron-dependent enzymes in the cytosol. Frataxin—the protein lacking in the neurological disease Friedreich's ataxia—functions as a mitochondrial iron chaperone for iron-sulfur cluster and heme biosynthesis (*8*, *9*).

Fungi are anomalous among eukaryotes in that they do not express ferritins. We expressed human H and L ferritins in the yeast *Saccharomyces cerevisiae*. The peptides assembled into multimeric complexes, with properties similar to those of native human ferritins, but contained only small amounts of iron (fig. S1, A and B). We hypothesized that yeast might also lack the requisite iron chaperones needed for delivery of iron to ferritin and designed a genetic screen to identify human genes that, when expressed in yeast, could increase the amount of iron loaded into ferritin. We introduced an iron-regulated *FeRE/HIS3* reporter construct (*10*) into a yeast strain expressing H and L ferritin (Fig. 1A). This construct confers histidine prototrophy to cells when the reporter is bound and transcriptionally activated by Aft1p, the major iron-dependent transcription factor in yeast. Aft1p is activated during periods of cytosolic iron depletion (*11*), which could occur if substantial amounts of cytosolic iron were diverted into ferritin.

Yeast cells containing ferritin and the iron-responsive reporter were transformed with a library synthesized from human liver cDNA engineered into a yeast expression vector. Transformants that exhibited growth on plates lacking histidine were selected for further analysis. We isolated multiple copies of PCBP1, as well as proteins encoded by other unrelated genes, including H ferritin. Plasmids containing PCBP1 or the empty vector were retransformed into reporter yeast strains lacking or expressing H and L ferritins (Fig. 1B). Expression of PCBP1 did not activate the *FeRE/HIS3* reporter in cells lacking ferritin, as indicated by a lack of growth on media without histidine. But expression of PCBP1 did activate the *FeRE/HIS3* reporter in the yeast strain expressing ferritins, resulting in growth on media lacking histidine. Thus, expression of human PCBP1 activated the iron-responsive reporter only in the presence of ferritin. To confirm that reporter activation was due to delivery of cytosolic iron into ferritin, we directly measured the incorporation of iron into ferritin by growing yeast in the presence of $[^{55}Fe]Cl_3$, isolating ferritin on nondenaturing gels, and measuring the amount of ^{55}Fe in the ferritin heteropolymer (Fig. 1, C and D). Substantial amounts of iron-containing protein were detected only in cells expressing ferritin, and iron was detected in a single species that comigrated with the ferritin heteropolymer. Coexpression of PCBP1 in these cells resulted in a 2.3-fold increase in the amount of iron in ferritin. This increase was not due to changes in the overall amount of ferritin (Fig. 1E) or in the relative ratio of H and L chains (fig. S1A). Similarly, the total amount of ^{55}Fe taken up by the cells expressing ferritin alone was not different from the amount taken up by cells expressing both PCBP1 and ferritin (fig. S1C).

The delivery of cytosolic iron to ferritin in the presence of PCBP1 activated the *FeRE/HIS3* reporter. We asked whether other proteins ex-

---

[1] Liver Diseases Branch, National Institute of Diabetes and Digestive and Kidney Diseases, National Institutes of Health, Bethesda, MD 20892, USA. [2] Department of Biochemistry and Molecular Biology, Wayne State University School of Medicine, Detroit, MI 48201, USA.

*To whom correspondence should be addressed. E-mail: carolinep@intra.niddk.nih.gov

requires the freezing of aqueous fluids. Water ice is likely to have formed in association with this process, appearing at temperatures near 0°C (*18*). If water ice melts, the brine composition approaches a chemical state essentially identical to the epsomite calculation described above, with an $a_{H_2O} = 0.78$ at epsomite and melanterite saturation.

Late-stage chloride precipitates have also been explored as vug precursor minerals on the basis of their relatively high solubility (*19*). Regardless of its identity, the dissolution of a chloride phase would require that infiltrating pore water became less saline, but still attained saturation with respect to Mg sulfate, with epsomite again fixing a_{H_2O} at 0.78.

Taken together, our results indicate that the evaporation of Meridiani groundwater led to a sustained $a_{H_2O} \leq 0.78$ to 0.86, values too low for all but a handful of terrestrial microorganisms to survive. Moreover, additional evidence suggests that chlorides are present in the sediments, pointing to still lower a_{H_2O} with continuing brine evolution. A range of Br/Cl ratios in different rocks suggests that highly soluble chlorides formed from evaporation and were incorporated into the wind-blown sediments (*4*, *19*). Progressive increases in Cl in rocks deeper in Endurance Crater suggest a similar process or one that differentially affected Cl during diagenesis (*19*). In addition, there is chemical and textural evidence for halite on rinds and rock coatings analyzed at Meridiani Planum, most likely reflecting late-stage fluid movement or remnants left when altering fluids finally evaporated to dryness (*23*). Accordingly, the maximum a_{H_2O} at chloride formation (0.48, Fig. 1) may reflect initial evaporite formation, syndepositional fluid chemistry, and/or very late-stage diagenesis.

On a planetary scale, Mars Odyssey Gamma Ray Spectrometer results show Cl-H_2O correlation across much of the martian surface (*24*), consistent with recent spectral evidence for widespread mid- to late-Noachian chloride-bearing lithologies in the southern highlands (*25*). Because late-stage martian brines would have evolved toward Cl-rich compositions as sulfates were precipitated (*20*), these observations probably represent the signature of low-a_{H_2O} brines. "Paso Robles"–class Fe-sulfate–rich soils at Gusev Crater represent another investigated locality characterized by extreme acidity and high salinity (*8*). Mössbauer and reflectance spectroscopic measurements, supported by α-proton x-ray spectrometer analyses, show that candidate Fe-sulfate minerals include ferricopiapite and rhomboclase (*8*, *26*, *27*). Mg sulfate is also indicated in some analyses, occurring as several percent $MgSO_4$ by weight. The a_{H_2O} for a Fe^{3+}-rich brine in equilibrium with ferricopiapite, rhomboclase, and epsomite is 0.61, with a pH (SOM text) of –0.7: a remarkably harsh environment uninhabitable by known microorganisms (*10*, *18*).

Some martian meteorites also contain evaporite assemblages of martian origin, most likely reflecting subsurface geochemical processes. Members of the nakhlite class have carbonate minerals, including siderite and magnesite, as well as gypsum and epsomite (*7*). The Nakhla meteorite also contains late-stage halite; its saline assemblage represents the highest recorded extent of evaporative concentration on Mars. This evaporite mineral assemblage can be generated from an acidic solution with the same cation proportions as at Meridiani Planum (setting an initial pH of 4.8 and a SO_4/Cl ratio of 2.05) (*20*). After siderite and gypsum precipitate, magnesite appears at an a_{H_2O} of 0.83, then epsomite at $a_{H_2O} = 0.78$. Halite precipitates at an a_{H_2O} of 0.40 (Fig. 1). These calculations imply that the a_{H_2O} of at least some fluids percolating through the martian subsurface dipped well below known limits of terrestrial habitability.

Our calculations suggest that a number of martian localities widely distributed in time and space hosted fluids that were 10 to 100 times more saline than halite-saturated terrestrial seawater. A number of terrestrial organisms have evolved mechanisms to accommodate the osmotic stresses imposed by high salinities (*28*). However, all known salt-tolerant organisms are descended from ancestors that could not survive low a_{H_2O}, indicating that although life has evolved mechanisms to stretch the envelope of habitability, such brines were not a cradle for life on Earth (*1*, *10*, *28*). Accordingly, life that could originate and persist in the presence of extremely low a_{H_2O} on Mars would require biochemistry distinct from any known in even the most robust halophiles on Earth.

Precipitation is the sedimentary signature of brines with low a_{H_2O}; dissolution records more dilute waters. Although more dilute solutions must have carried ions to the sites where Meridiani salts precipitated, there is little evidence locally that subsequent water table regeneration introduced groundwaters dilute enough to dissolve Mg-sulfate minerals. Globally, we cannot rule out the possibility that more habitable waters existed elsewhere on the planet or in the earliest epoch of martian history. However, empirical evidence for dilute water at the martian surface remains meager. Geochemical constraints on Meridiani diagenesis suggest that the process was limited by the availability of water (*29*), which is consistent with a global surface geochemistry controlled for more than 3.5 billion years by water-limited processes (*30*). At the same time, hydrological models suggest that Meridiani Planum was one of the few regions on Mars likely to be characterized by groundwater upwelling about four billion years ago (*31*). This slow, global-scale deep hydrology would have focused water/rock interactions on the subsurface, leading to chemically distinct, concentrated groundwaters (*31*). When migrating groundwater breached the surface, continued upwelling and evaporation would have allowed standing water bodies to evolve toward greater ionic concentrations while keeping total fluid volume more or less constant. Concentrated standing water left its mark at Meridiani Planum in the form of diagnostic subaqueous cross-beds (*2*, *4*, *5*), and these same rocks display some of the highest MgO and SO_3 abundances measured, implying Mg-sulfate saturation and low a_{H_2O}. Moreover, the search for larger, more dilute bodies of water earlier in the Noachian has proven difficult (*25*, *32*). New observations have abbreviated the era when dilute surface waters could have been more common, pushing it further into Mars' planetary infancy.

Observations at Meridiani and other salt-bearing localities, then, may not reflect snapshots taken as local Mars waters evaporated to dryness, but rather a long surface history dominated by rock instead of water. On a planet where saline minerals were continuously recycled at the surface instead of removed by subduction and plate tectonics, dilute fluids may have been transient exceptions. The sobering conclusion is that Meridiani Planum, an extreme environment in terms of terrestrial habitability, may have been among the last, best places for life on the early martian surface.

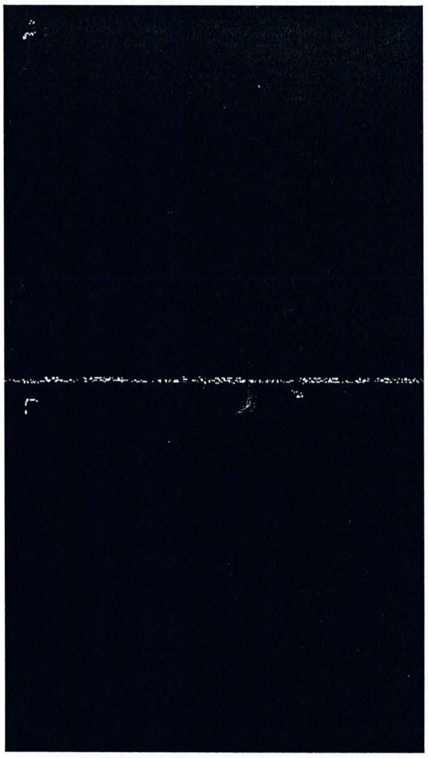

Fig. 2. Microscopic images taken by the Mars Exploration Rover Opportunity in Endurance Crater. (**A**) Portion of image taken of the undisturbed surface of Cobble Hill on martian day (sol) 144. (**B**) Portion of a mosaic taken on sol 149 of the feature London after being ground with the rock abrasion tool (RAT). Distinct grain boundaries are observable throughout both images. Primary laminations (a) and bedding structures are clearly visible. Secondary moldic porosity (b) can be seen throughout the RAT-abraded target, providing evidence for the selective removal of a syndepositionally formed soluble mineral while preserving primary sedimentary fabric. These features, observable in most places throughout Meridiani outcrop rocks, suggest groundwater saturation with respect to a Mg-sulfate phase during diagenesis. Secondary recrystallization is evident in some places, as shown by a generation of cement (c) surrounding hematitic concretions (d). Scale bars, 5 mm.